The Ocean*

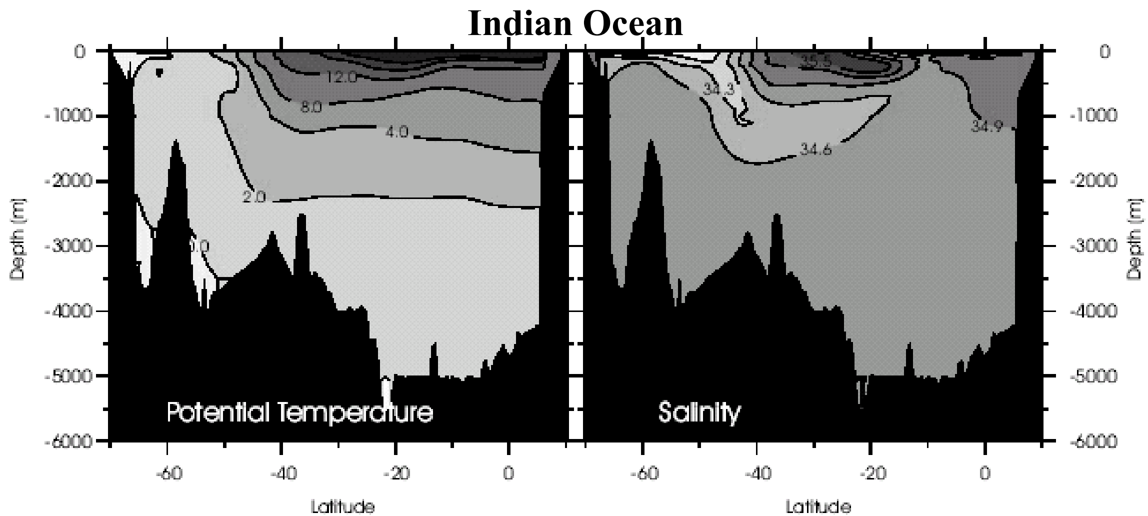

Koltermann et al. (2005)

There are a number of good books dealing with the ocean. At a level appropriate to this class: Bigg, G., 2003, *The Oceans and Climate*, 2nd Ed., Cambrige University Press, 273 pp.; Pickard, G.L. and W.J. Emery, 1990, *Descriptive Physical Oceanography*, 5th Ed., Pergamon Press, Oxford, 320 pp.; Pond, S. and G.L. Pickard, 1983, *Introductory Physical Oceanography*, Pergamon Press, Oxford, 329 pp. On a more mathematical level: Pedlosky, J., 2004, *Ocean Circulation Theory*, Springer, 453 pp.

* These notes are partly based on material kindly provided by **Christof Appenzeller**, MeteoSwiss.

The world oceans

The global ocean is considered as consisting of the following basins (definition of the boundaries may slightly vary):

- Arctic Ocean > 65° N;
- Atlantic Ocean 30° S - 65° N, 20° E - 70° W;
- Indian Ocean 30° S - 65° N, 20° E - 120° E;
- Pacific Ocean 30° S - 65° N, 120° E - 70° W;
- Southern Ocean < 30° S .

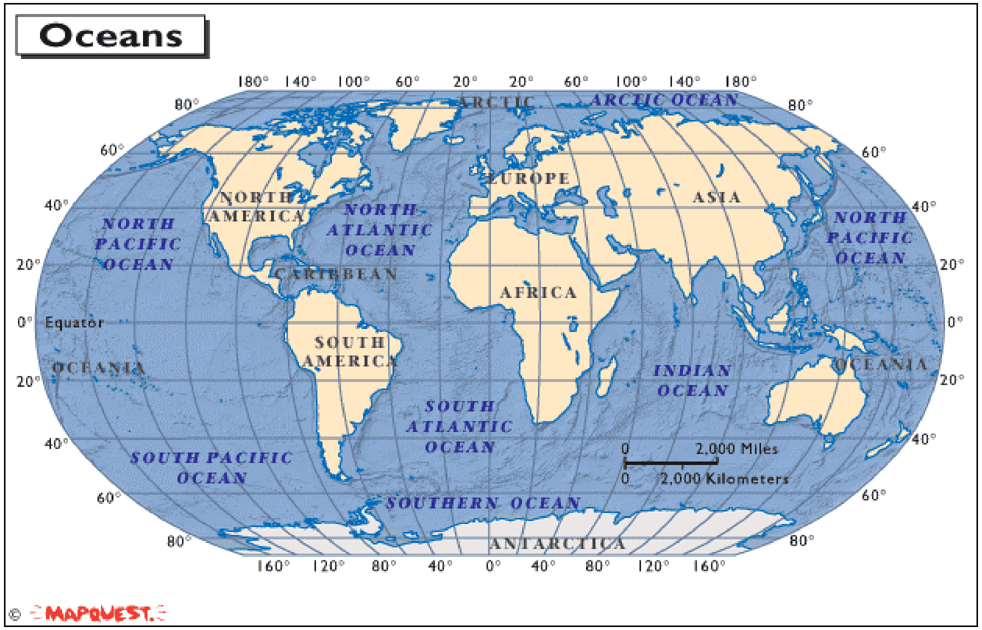

http://go.hrw.com/atlas/norm_htm/oceans.html

Characteristics of the world oceans

From the gridded 0.5 × 0.5° WGHC climatology and the ETOPO5 data sets mean properties have been calculated.

Ocean	T [°C]	Θ [°C]	Salinity	Oxygen [ml/l]	Silicate [μmol/kg]	Nitrate [μmol/kg]	Phosphate [μmol/kg]	σ_0 [kg/m^3]	Area [km^2]	Volume [km^3]
Global	3.8142 *5574382*	3.6460 *5574382*	34.7229 *5569065*	3.9199 *5571225*	88.1835 *5564439*	31.2087 *5563021*	2.1670 *5562954*	27.4865 *5564798*	360808032 *171071*	1298060310 *5574382*
Arctic	–0.1945 *618393*	–0.2642 *618393*	34.7139 *617961*	6.9427 *617857*	9.7787 *617048*	13.1146 *617610*	0.9546 *617672*	27.8805 *618405*	13340939 *25647*	16630286 *618393*
Atlantic	4.2636 *1309580*	4.0882 *1309580*	34.9352 *1305908*	5.1149 *1307049*	44.3891 *1306020*	22.8536 *1303442*	1.5842 *1303308*	27.6002 *1298226*	92846458 *40626*	322453728 *1309580*
Indian	3.9864 *969300*	3.8270 *969300*	34.7552 *968087*	4.0027 *967187*	88.9434 *967062*	31.7037 *966744*	2.2233 *966751*	27.4795 *968333*	68163250 *27936*	247991233 *969300*
Pacific	3.6437 *2677109*	3.4733 *2677109*	34.6154 *2677109*	3.2781 *2679132*	109.6173 *2674309*	35.2450 *2675225*	2.4398 *2675223*	27.4283 *2679834*	186457385 *76839*	710985063 *2677109*
Southern	2.5894 *2003778*	2.4363 *2003778*	34.6382 *2003778*	4.7451 *2050272*	84.3408 *2001718*	30.7932 *2000858*	2.1298 *2000721*	27.5913 *1992319*	10796981 *57823*	403406857 *2003778*

*) The number of affected grid-nodes is given in italics. Areas are calculated assuming a spherical earth with the radius of 6371 km. The ETOPO5 bathymetry at the resolution of the climatology, that is 0.5° × 0.5°, is used for these calculations of areas and volumes.

* Koltermann, K.-P., J. Meincke and V. Gouretski, 2005, *Global Ocean and Sea Ice*. In: Hantel., M. (Ed.), Observed Global Climate, *Landolt-Börnstein*, V/6 (Geophysics/Climatology), Springer.

The ocean in the climate system

The world oceans:

- cover roughly 70 % of the earth's surface;
- represent roughly 97 % of the water storages;
- represent therefore about 97 % of the mass contained in the biosphere/atmosphere/cryosphere/hydrosphere.

Due to the high thermal capacity of water (specific heat of 4187 J kg^{-1} K^{-1} for pure water as compared to 1004 J kg^{-1} K^{-1} for dry air), the world oceans can store and transport a considerable amount of heat.

As a result, seasonal variations in the sea surface temperature (SST) are modest, not exceeding 8 °C. In contrast, seasonal excursion of the surface temperature over the land masses can reach 50 °C.

The energy balance of the surface waters

Consideration the <u>energy balance of the surface layer</u> is essential for understanding how the oceans are heated. Note that we really look at a volume, not just at the surface itself.

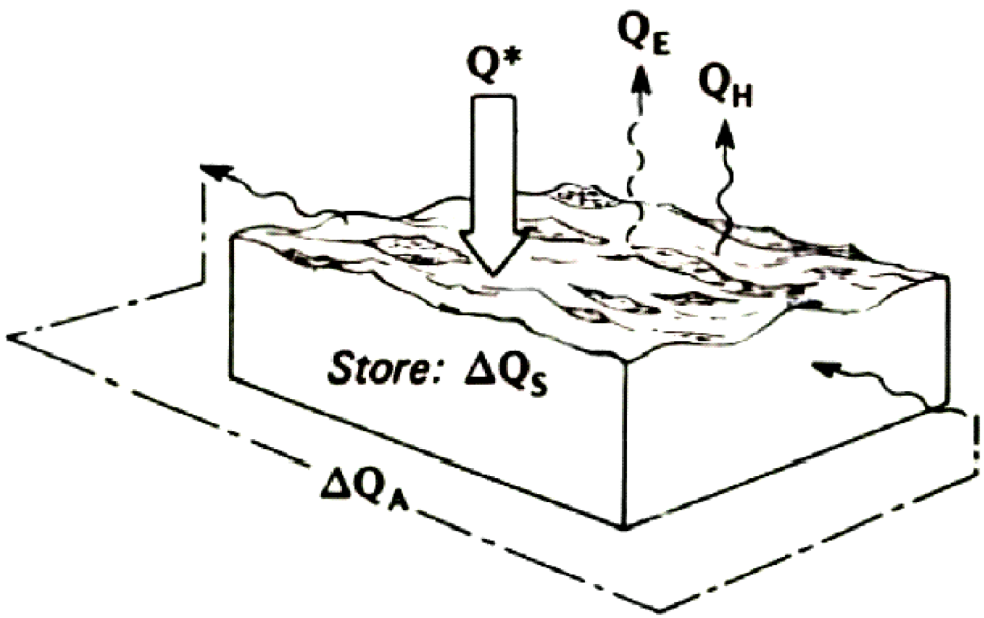

$Q^* = NR$
$Q_H = H$
$Q_E = L_v E$
$QG = G$
$\Delta Q_S = \Delta S$

Figure 3.14 Schematic depiction of the fluxes involved in the energy balance of a water volume.

Oke (1987)

Energy fluxes

The energy budget of the oceans is peculiar. An excess of solar radiation during the day, partly due to the low albedo of water at moderate solar zenith angles, leads to heating of the underlying water. During night, heat is released to the atmosphere through the fluxes of sensible and latent heat.

Note that the average Bowen ratio of the oceans is close to 0.1.

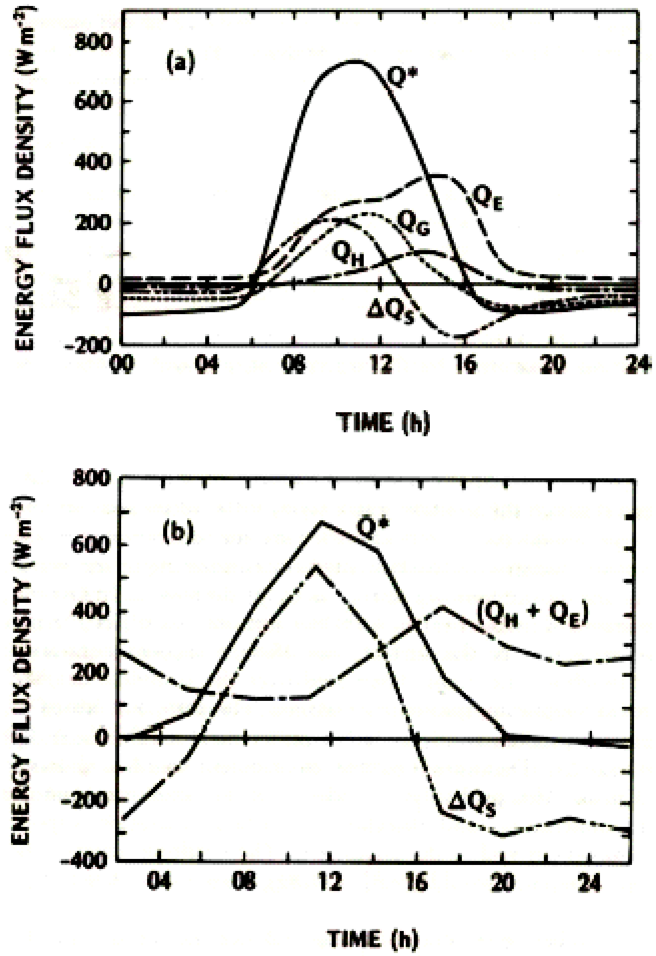

Figure 3.15 Diurnal variation of the energy balance components in and above (a) a shallow water layer on a clear September day in Japan (after Yabuki, 1957), and (b) the tropical Atlantic Ocean based on measurements from the ship *Discoverer* in the period 20 June to 2 July 1969 (after Holland, 1971).

Oke (1987)

The albedo of water

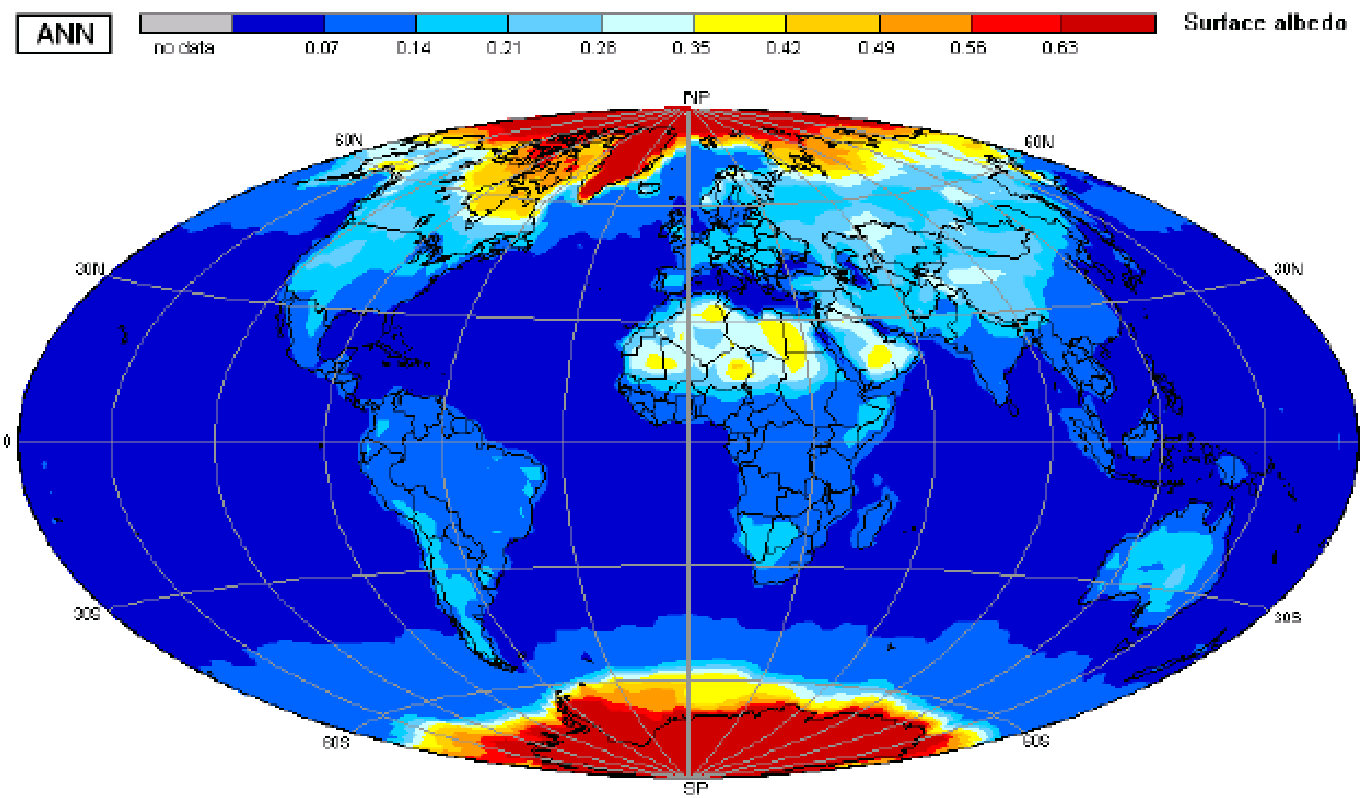

Fig. 4.3.4.13 Annual average of the effective values of the surface albedo of the earth for solar radiation during the period 1991 to 1995, in Wm^{-2}. These fields result from various assumptions on the real albedo and their increase with increasing zenith angle of the Sun, and on operational reports of snow and ice cover. Lowest values over the ocean for Sun at zenith are 0.06 and highest values over the polar snow and ice fields are 0.7. Highest and lowest values: 0.80 and 0.07; global average: 0.13. The albedo of the water was modeled with some dependence on the solar zenith angle, cloud amount and the wind speed.

Raschke and Ohmura (2005)

Calanca, 30.05.2006

The albedo of water for direct solar radiation

For solar zenith angles of less than about 70° (solar elevations of more than 20°), the albedo of a plane water surface is small, typically less than 0.15, but increases very rapidly for zenith angles above this threshold.

albedo

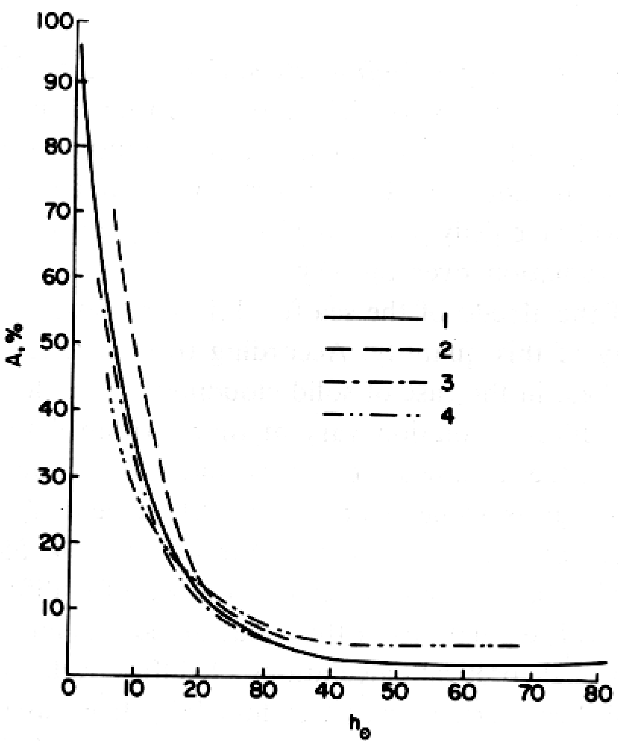

solar elevation

Kondratyev (1969)

Calanca, 30.05.2006

The albedo of water for direct solar radiation (2)

The dependence of the albedo of water on solar elevation can be explained with the help of Fresnel's formula (List, 1984). Namely, the reflectivity of a plane water surface for unpolarized light is given by:

$$\alpha_{wat} = 0.5 \cdot \left[\frac{\sin^2(i-r)}{\sin^2(i+r)} + \frac{\tan^2(i-r)}{\tan^2(i+r)} \right]$$

where i denotes the angle of the incident beam (zenith angle of the sun), and r is the angle of refraction given by Snell's law as:

$$\sin(r) = \frac{n_{air}}{n_{wat}} \cdot \sin(i)$$

$n_{air} = 1.00$ and $n_{wat} = 1.33$ are the refractive indices of air and water, respectively.

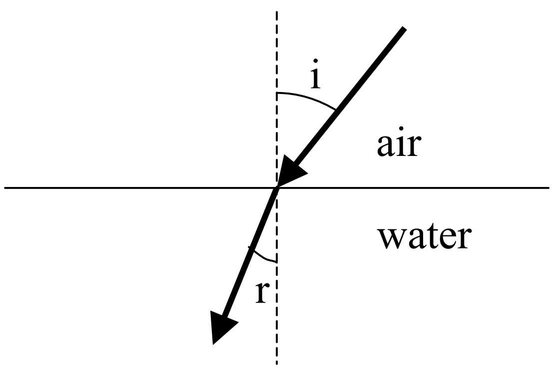

The albedo of water revisited

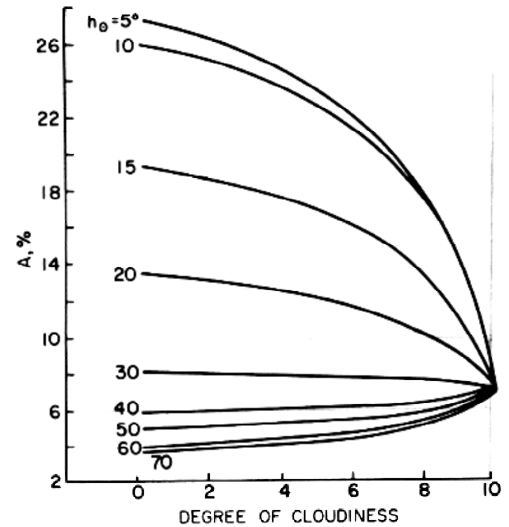

FIG. 7.12 *Water albedo at different solar heights z and cloudiness degrees for global radiation.*

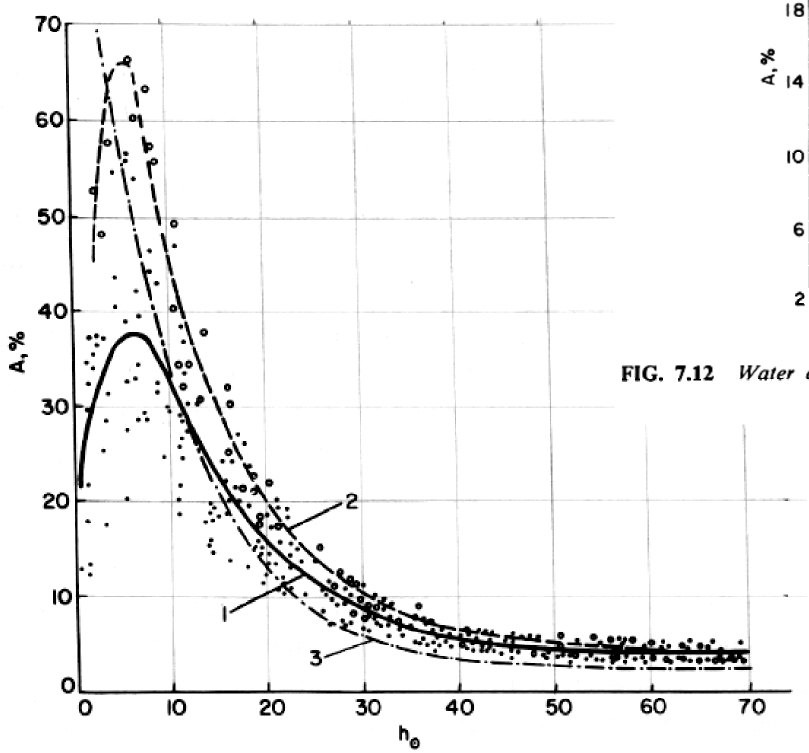

FIG. 7.11 *Dependence of the sea surface albedo upon solar height.*

Kondratyev (1969)

Extinction of solar radiation

The extinction of solar radiation in water can be well approximated by the Beer-Bouguer-Lambert law. The extinction coefficient depends on the chemical make-up of the water (turbidity, that is the amount of suspended material, plankton, ...) and increases with wavelength toward the infrared (red light absorbed more rapidly than blue light).

In most water bodies shortwave radiation is restricted to the uppermost 10 m, but in some very clear tropical waters it has been observed to reach 700 to 1000 m.

Seasonality of the surface temperature

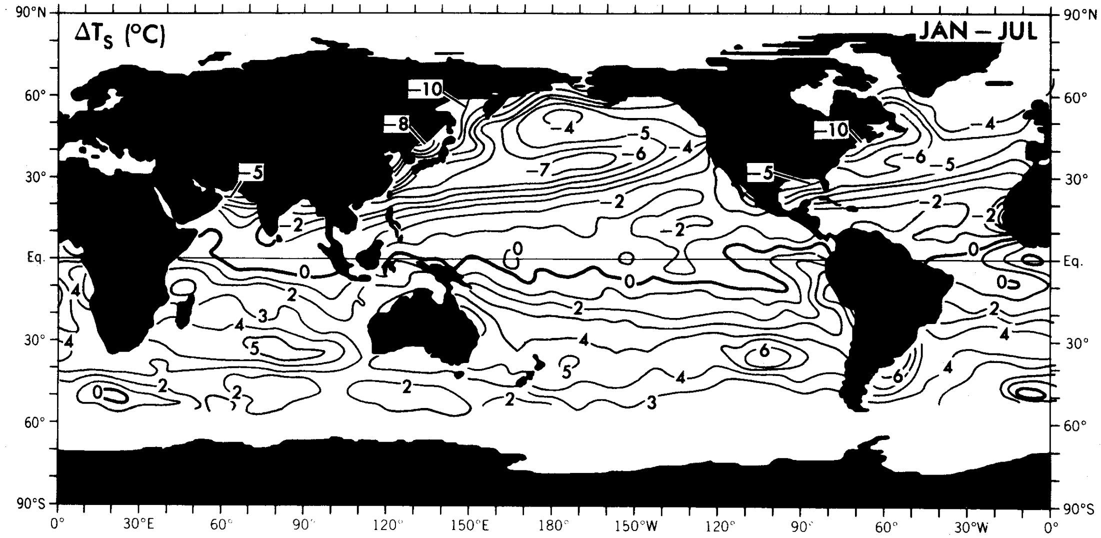

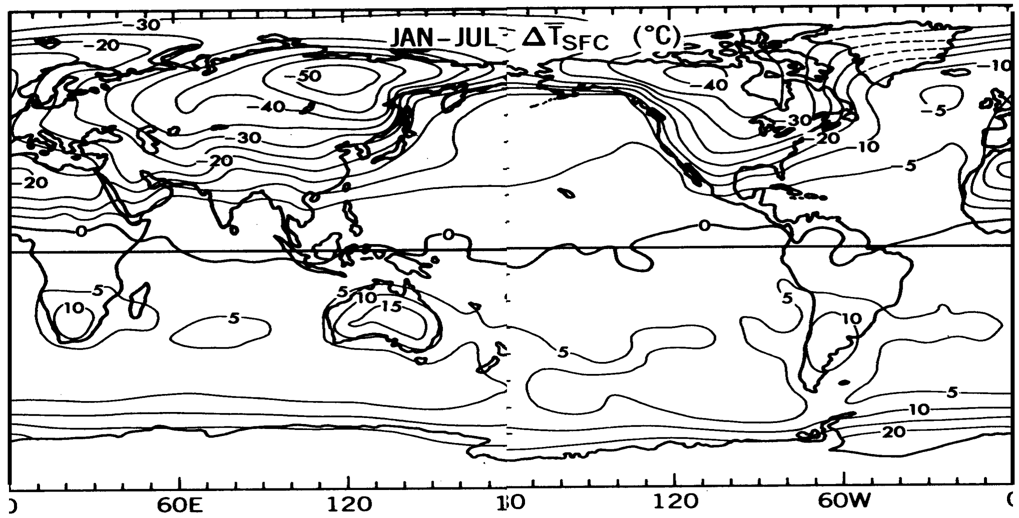

After Peixoto and Oort (1992)

Meridional transport of energy in the climate system

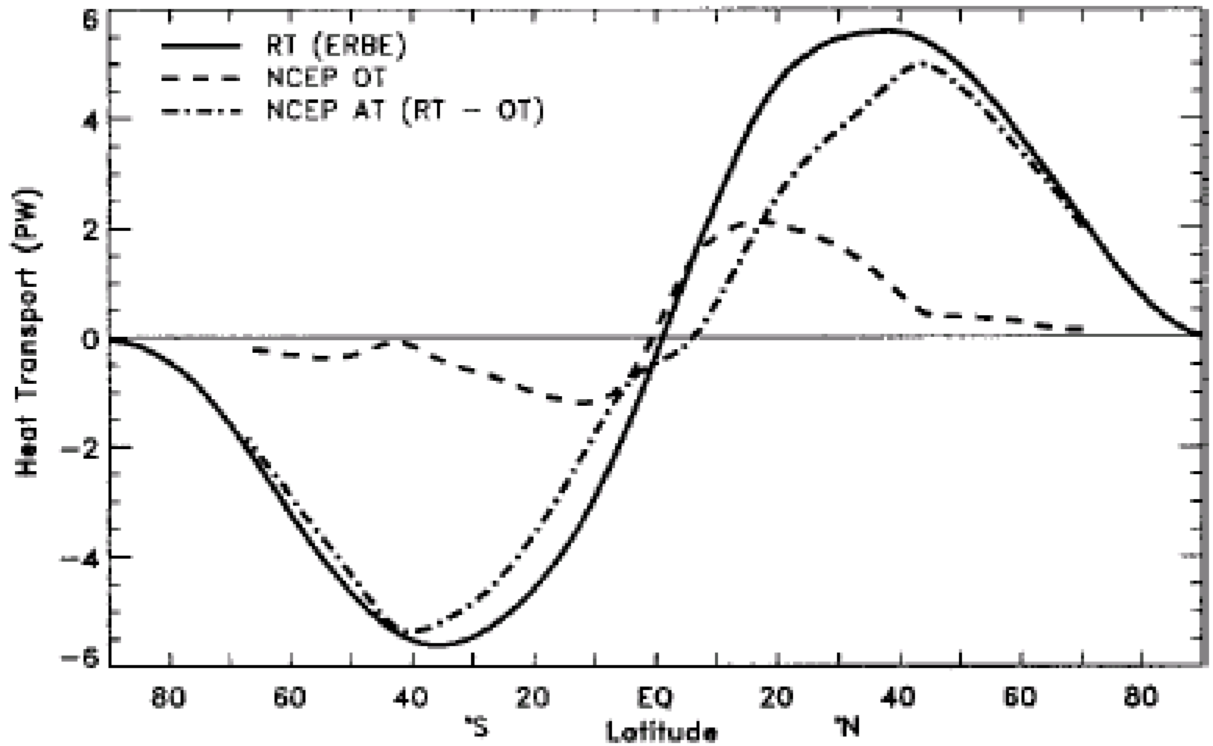

FIG. 7. The required total heat transport from the TOA radiation RT is compared with the derived estimate of the adjusted ocean heat transport OT (dashed) and implied atmospheric transport AT from NCEP reanalyses (PW).

Trenberth, K.E. and J.M. Caron, 2001: Estimates of meridional atmosphere and ocean heat transports. *J. Climate*, **14**, 3433-3443.

Storage of carbon

Due to the high solubility of CO_2 in water, the deep water can store a considerable amount of carbon.

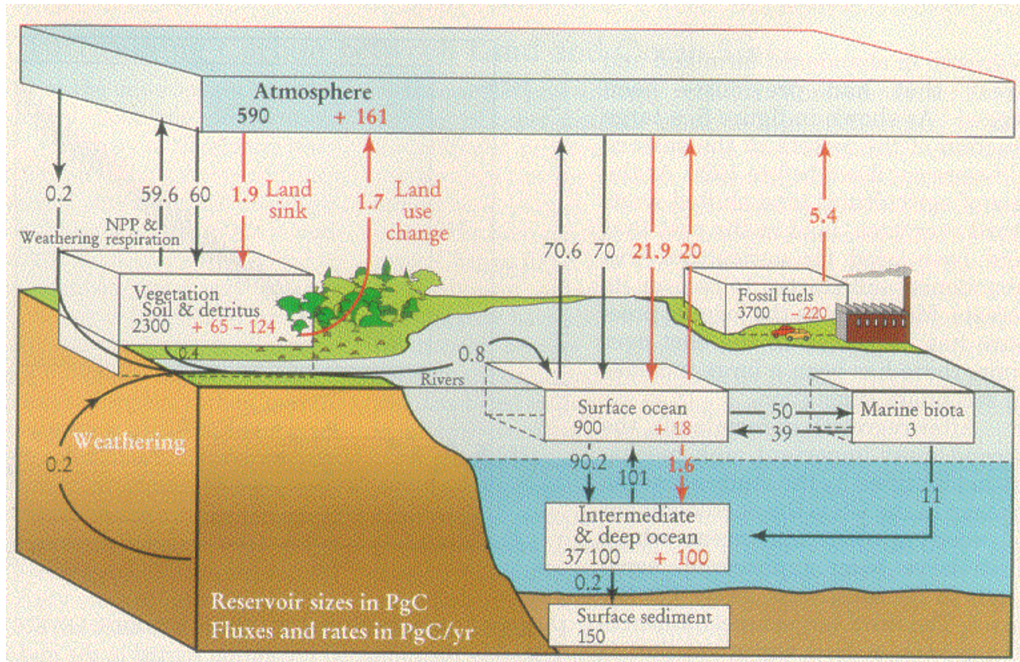

FIGURE 1. GLOBAL CARBON CYCLE. Arrows show the fluxes (in petagrams of carbon per year) between the atmosphere and its two primary sinks, the land and the ocean, averaged over the 1980s. Anthropogenic fluxes are in red; natural fluxes in black. The net flux between reservoirs is balanced for natural processes but not for the anthropogenic fluxes. Within the boxes, black numbers give the preindustrial sizes of the reservoirs and red numbers denote the changes resulting from human activities since preindustrial times. For the land sink, the first red number is an inferred terrestrial land sink whose origin is speculative; the second one is the decrease due to deforestation.[16] Numbers are slight modifications of those published by the Intergovernmental Panel on Climate Change.[3] NPP is net primary production.

Sarmiento and Gruber (2002)

1 Pg (petagram) $\equiv 10^{15}$ g $\equiv 10^{12}$ kg

Carbon dioxide solubility

Carbon dioxide, like other gases, is soluble in water. Its <u>solubility</u>, $\sigma_{CO2}(S,T)$, that is the saturation concentration divided by the atmospheric partial pressure, is a function of salinity and temperature. For a given salinity, <u>solubility increases with decreasing temperature</u>, as shown in the following picture.

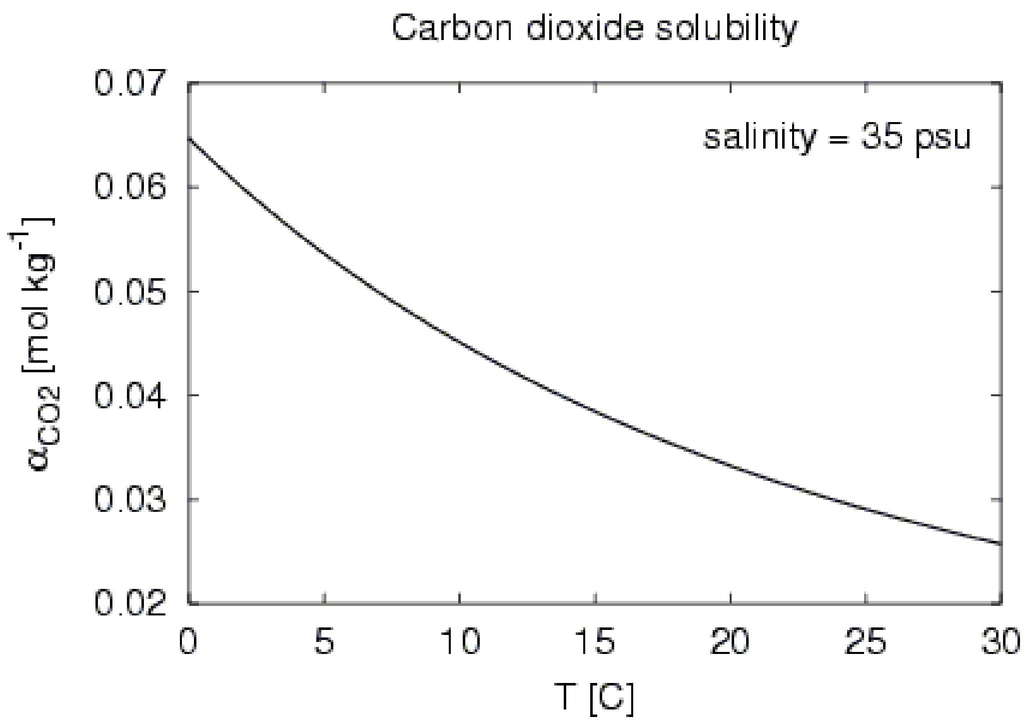

Carbon dioxide in the ocean

Unlike many other gases (oxygen for instance), CO_2 reacts with water and forms a balance of several ionic and non-ionic species (collectively known as dissolved inorganic carbon, or DIC). These are dissolved free carbon dioxide (CO_2), carbonic acid (H_2CO_3), bicarbonate (HCO_3^-) and carbonate (CO_3^{2-}), and they interact with water as follows:

$$CO_2 + H_2O \leftrightarrow H_2CO_3 \leftrightarrow HCO_3^- + H^+ \leftrightarrow CO_3^{2-} + 2\,H^+$$

As pointed out by Bigg (2003), the component reactions are fast, but the conversion of bicarbonate to carbonate proceeds at a speed roughly 1000 times slower than the conversion of carbon dioxide into bicarbonate. The net effect is therefore a summary reaction given by:

$$CO_2 + H_2O + CO_3^{2-} \leftrightarrow 2HCO_3^-$$

The bicarbonate/carbonate species are not produced solely from the equilibrium with CO_2, but also have source from deposition (river or wind-blown dust) and weathering. These background sources permits a greater absorption of atmospheric CO_2 than would otherwise occur.

Uptake of carbon dioxide by the ocean

It is usually assumed (Broecker and Peng, 1982) that the <u>flux of CO_2</u> at the sea/atmosphere interface is proportional to the difference in concentration between a thin diffusive layer beneath the surface , $[CO_2]_{sf}$, and the lower boundary of the mixed layer, $[CO_2]_m$, the proportionality constant λ being essentially dependent on the surface wind speed. Defining the z-axis positive upward we have:

$$F_{CO_2} = -\lambda(U)\cdot\left([CO_2]_{sf} - [CO_2]_{ml}\right)$$

The concentration in the surface layer can be expressed in terms of the solubility, $\sigma_{CO2}(T,S)$, and the partial pressure in the atmosphere, p_{CO2}:

$$[CO_2]_{sf} = \sigma_{CO2}\cdot p_{CO2}$$

Since the atmospheric concentrations as well the partial pressure of CO_2 are roughly uniform over the globe, the above equations show that the direction of the flux of CO_2 at the sea/atmosphere interface depends on whether the oceanic concentration is above/below the <u>equilibrium concentration</u>. Due to the temperature dependence of the solubility this occurs in the tropics/high latitudes.

Uptake of carbon dioxide by the ocean (2)

Thus, on an annual mean, the Arctic regions represent a sink of atmospheric CO_2, while the equatorial and sub-tropical regions are a source (Takahashi et al., 1997)

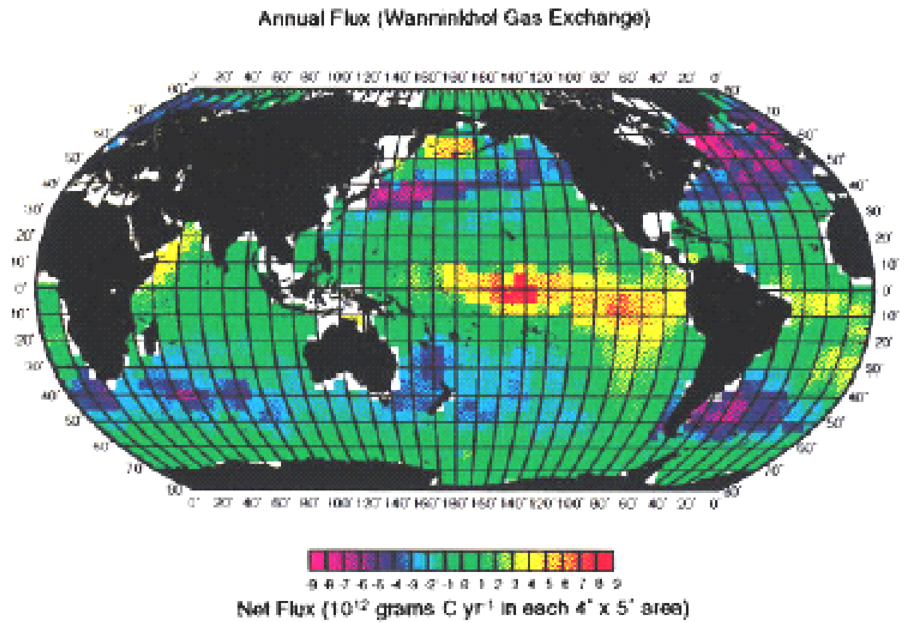

FIG. 5. Mean annual net CO_2 flux over the global oceans (in 10^{12} grams of C per year for each pixel area) computed for 1990 using the gas transfer coefficient formulated by Wanninkhof (70). The effect of full atmospheric CO_2 increase is assumed for normalizing observed ΔpCO_2 values in high latitude areas to the reference year of 1990. Areas covered with ice (i.e., the poleward of the pink lines in Figs. 4 *a* and *b*) are assumed to have zero sea–air CO_2 flux.

* Takahashi, T. et al., 1997, Global air-sea flux of CO2: An estimate based on measurements of sea–air pCO2 difference, *Proc. Natl. Acad. Sci. USA,* Vol. 94, pp. 8292–8299.

The ocean as a source of water vapor

The oceans also represent a major <u>source of water vapor</u> for the atmosphere.

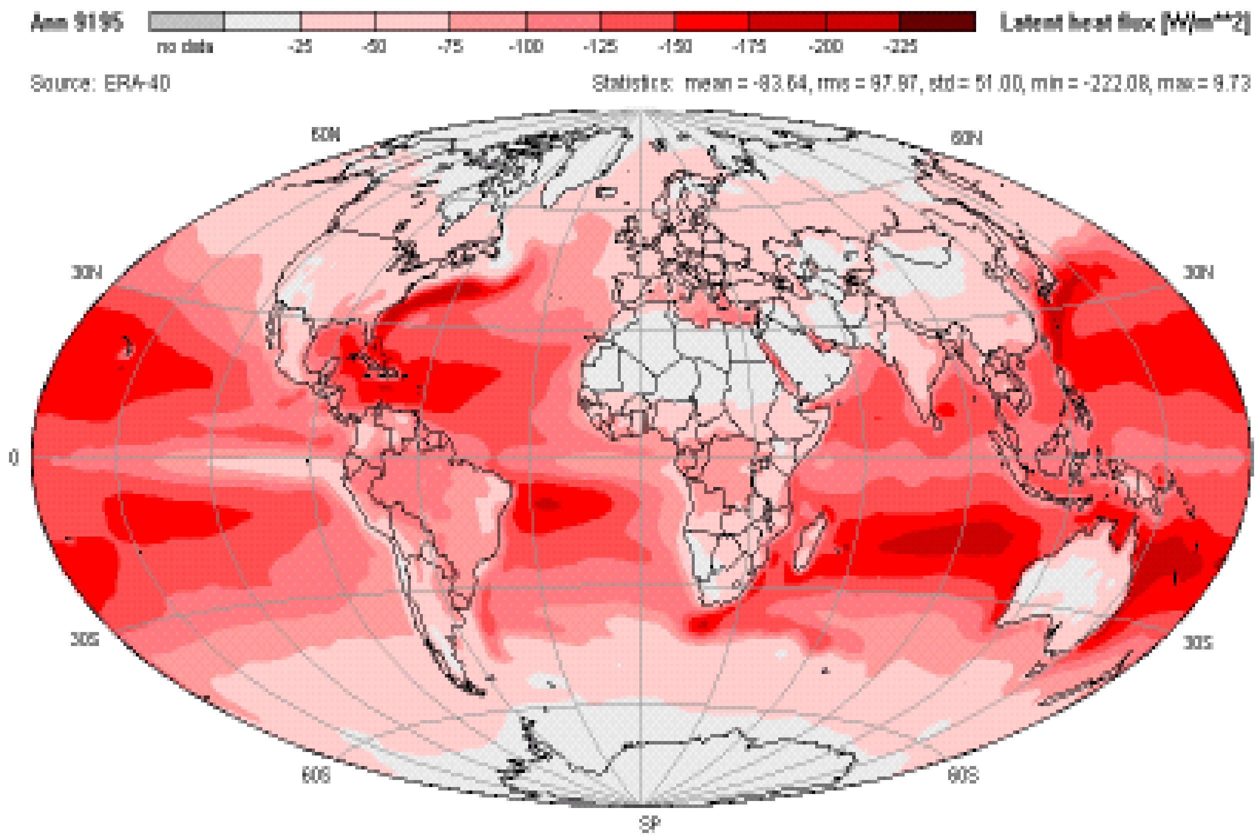

Fig. 10.3b Annual mean distribution of **latent heat fluxes**, based on data of the re-analysis project ERA-40. This data set covers the period 1991-1995.

Ohmura and Raschke (2005)

Salinity of seawater

Seawater contains a quantity of dissolved material (mostly ions) collectively termed salinity (see Table below). The average salinity of the oceans is about 35 g kg^{-1} or 35 ‰ or 35 psu*.

Concentrations of the Major Components of Seawater with a Salinity of 35‰

Component	Grams per kilogr
Chloride	19.353
Sodium	10.76
Sulfate	2.712
Magnesium	1.294
Calcium	0.413
Potassium	0.387
Bicarbonate	0.142
Bromide	0.067
Strontium	0.008
Boron	0.004
Fluoride	0.001

Hartmann (1994)

* Since 1982 a salinity scale based on the electrical conductivity of sea water has been used. In this system, salinity is expressed in practical salinity units (psu). Salinity values in psu units are essentially identical to a measure of parts per thousand (‰) by weight

Salinity of the world oceans

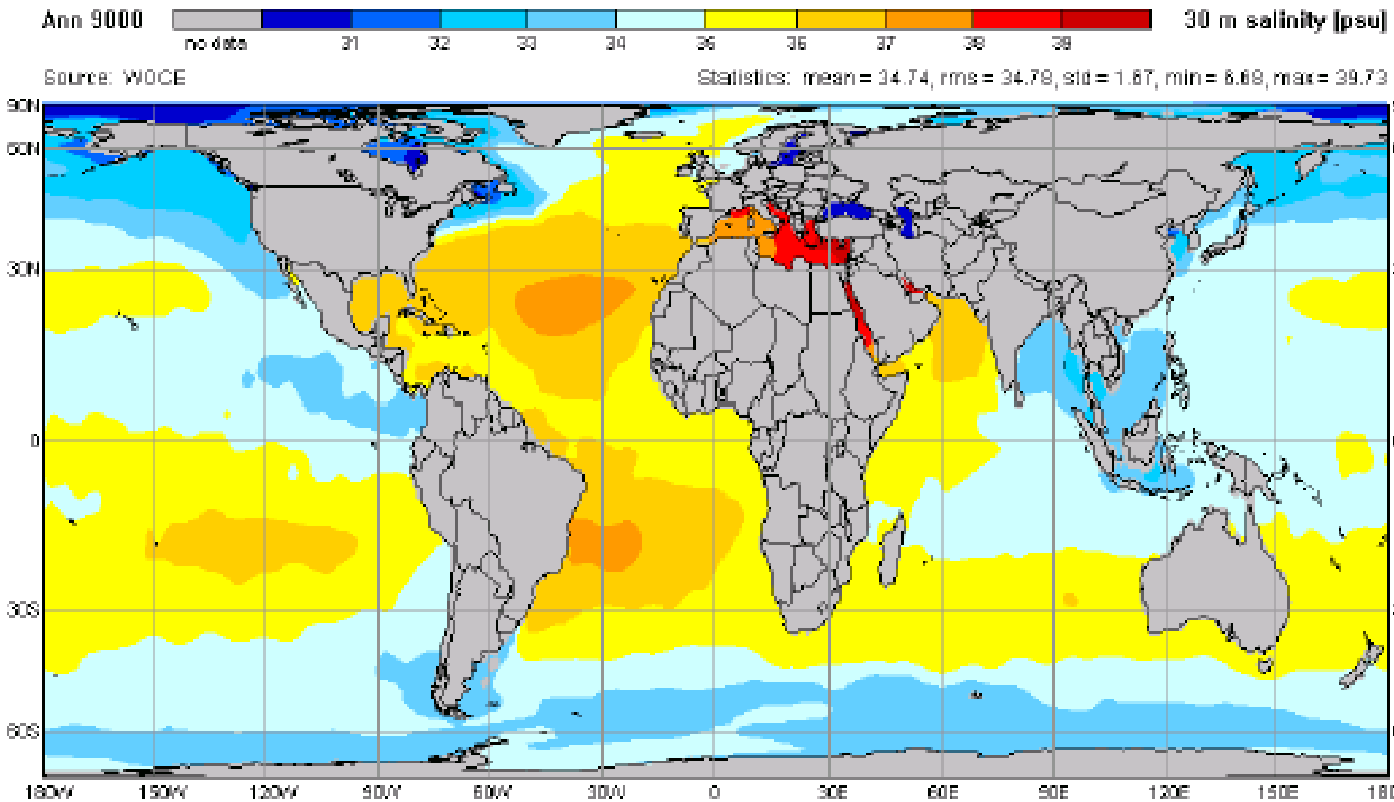

Fig 14.16 Global distribution of salinity at 30 m depth in the global ocean based on the WGHC climatology

Koltermann et al. (2005)

Salinity of the world oceans (2)

Salinity can vary considerably with depth, as seen in the following cross-sections taken across the Atlantic and Pacific Oceans.

14.3.2.1 The Atlantic Ocean (20 W)

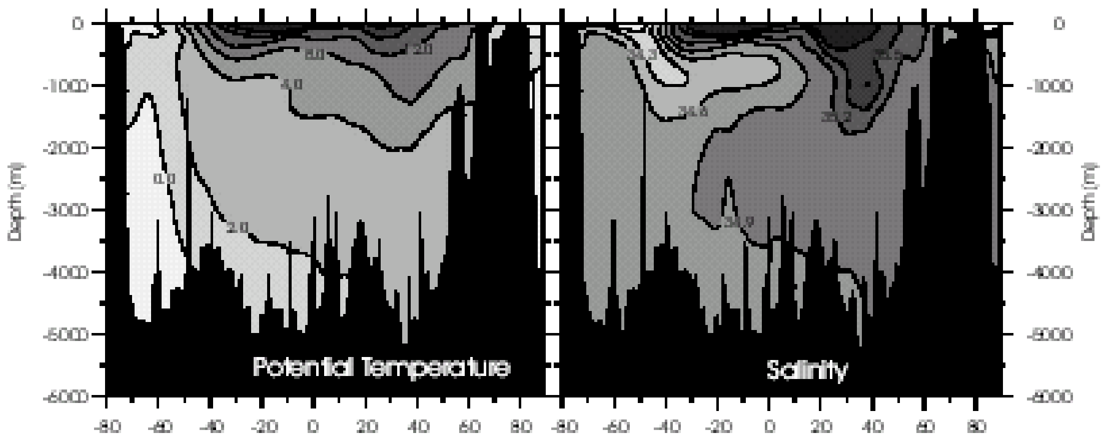

14.3.2.3 The Pacific Ocean (170 W)

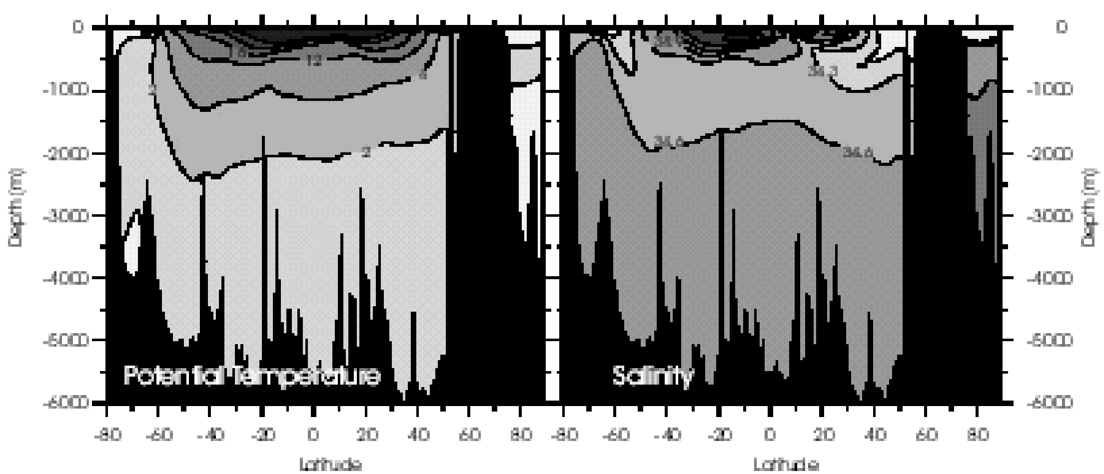

Koltermann et al. (2005)

Density of sea water

The global circulation in the world oceans, the thermohaline circulation (see later on), are driven by density gradients. The density of sea water, ρ(T,S,p), depends on both temperature (T) and salinity (S) and, to a negligible degree, on pressure (p).

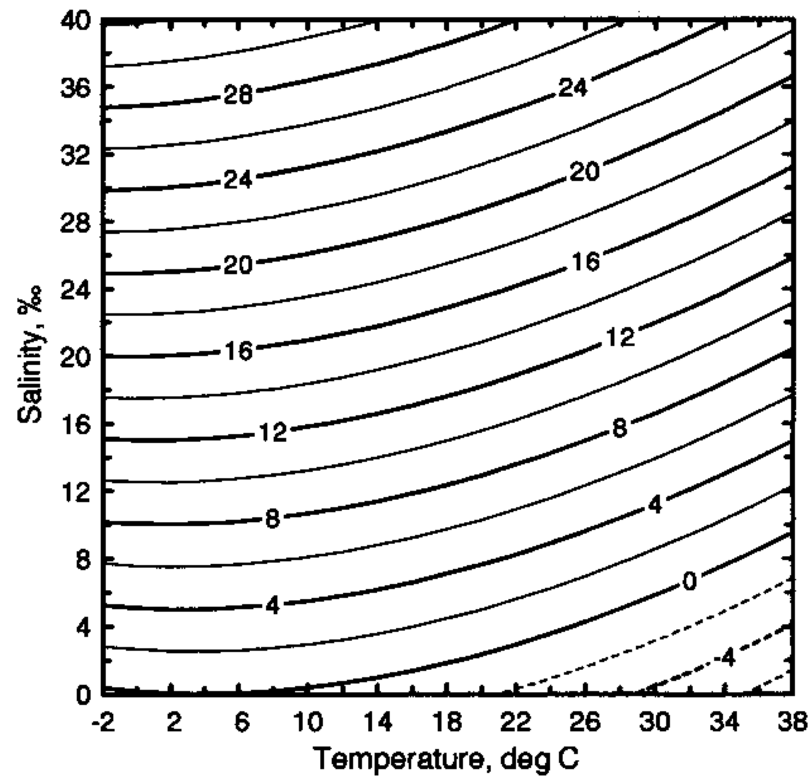

Density anomaly, $\rho - 1000$ [kg m^{-3}], as a function of temperature and salinity. From Hartmann (1994).

Density of sea water (2)

TABLE 2.1 *Values of density* in situ *for fresh and sea water* ($kg\,m^{-3}$) (*International Equation of State* 1980)

Sea pressure	Approx. depth	Fresh water S = 0 temperature		Average sea water S = 35 temperature		Red Sea (winter) S = 40 temperature
10^2 kPa	m	0°	30°C	0°	30°C	18°C
0	0	999.8	995.7	1028.1	1021.7	1029.1
10	100	1000.4	996.1	1028.6	1022.2	1029.6
100	1000	1004.9	(1000.0)	1032.8	(1026.0)	1033.4
400	4000	(1019.3)	(1012.7)	1046.4	(1038.1)	1045.8
1000	10 000	(1045.3)	(1035.9)	1071.0	(1060.4)	(1068.7)

Pond and Pickard (1983)

The thermocline

The most prominent feature in the vertical distribution of the temperature is certainly the thermocline, a sharp decline in temperature over a very shallow layer. We distinguish between the seasonal thermocline, usually found at a depth of ~ 100 m (left panel), and the permanent thermocline, located at depths of ~ 1000 m (right panel)..

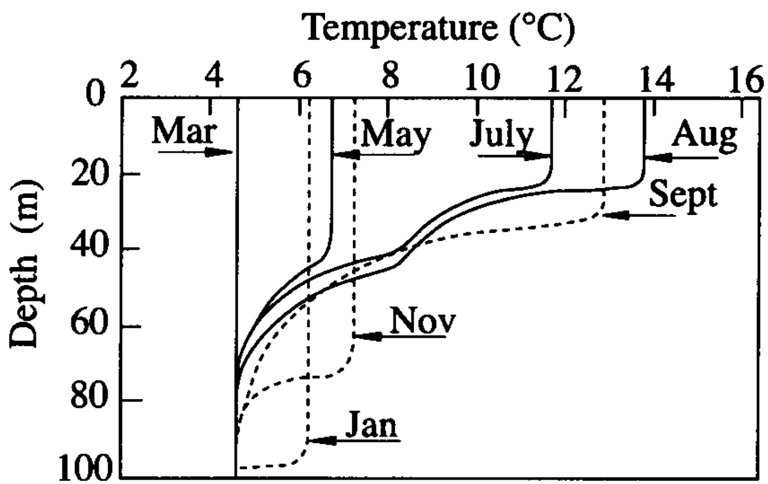

Evolution of the temperature in the upper 100 m
of the Pacific Ocean (50°N, 145°W) (Hartmann, 1991).

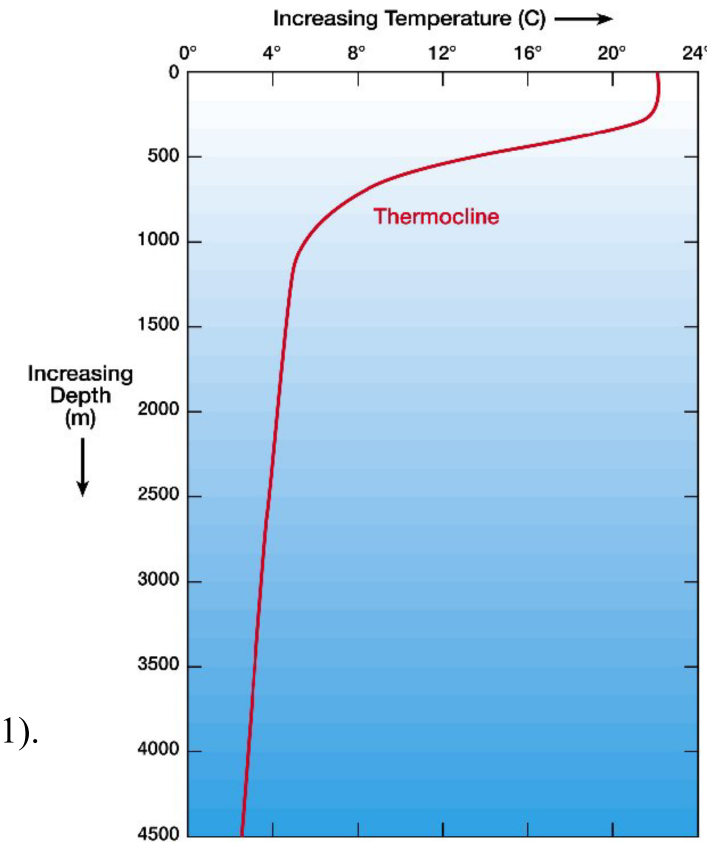

The thermocline and salinity

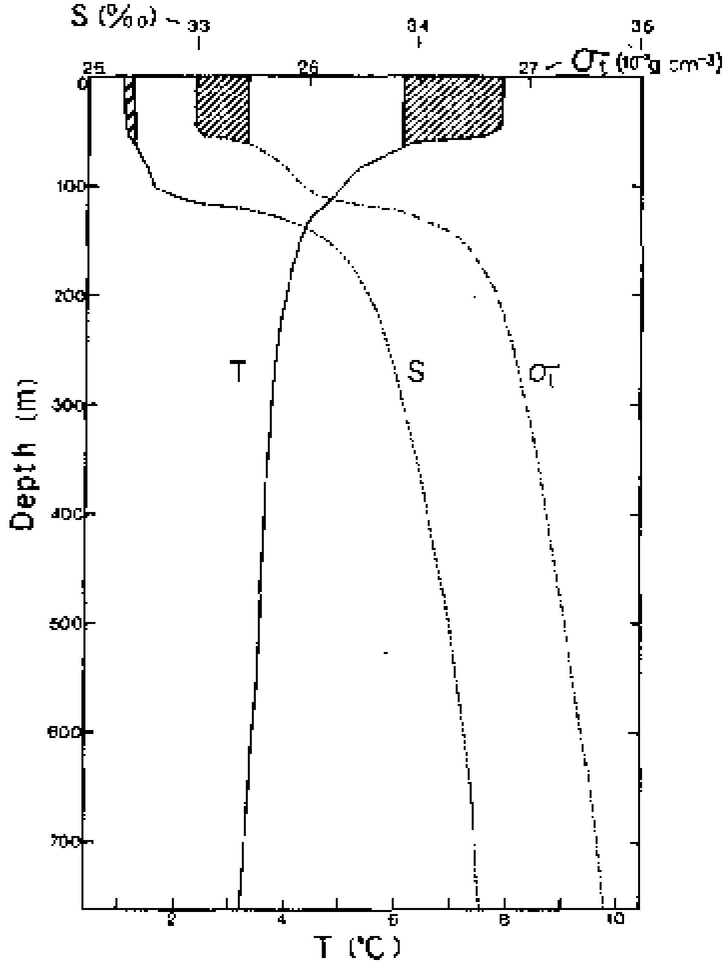

FIG. 1. An STD trace taken at Station *Papa* at 2100 GMT 23 June 1970. The hatched areas represent the change in T, S and σ_t that occurred since 19 May 1970.

Denman and Mikaye (1973)

Currents in the oceans

In dealing with the oceanic currents it is convenient to distinguish among the following types of circulations:

- Wind-driven circulation. This takes place in the mixed layer, on scales ranging from the local to the global, and consists of both a horizontal as well as vertical component;
- The gyres. These are mainly horizontal currents on the large scale. The so-called boundary currents on the western side of the gyres are part of this type of circulation;
- The thermohaline circulation. It is driven by the large-scale density gradients, which themselves depend of the distribution of temperature (→ thermo) and salinity (→ haline). After Broecker (1987), the thermohaline circulation is often associated to the global conveyor belt, but the concept is controversial (see e.g. Rahmstorf, 1999).

Rahmstorf, S., 1999, Currents of Change, Investigating the Ocean’s Role in Climate. Essay for the McDonnell Foundation Centennial Fellowship.

Wind-driven circulation

Atmospheric winds exert a drag or stress on the sea surface, according to:

$$\vec{\tau} = \rho C_D \left\|\vec{U}\right\| \vec{U}$$

where ρ is the air density, U is the wind vector, and C_D a drag (bulk exchange) coefficient that itself is a function of the wind speed and the surface roughness. The equation shows that the stress is parallel to the surface wind, which leads to the following picture of

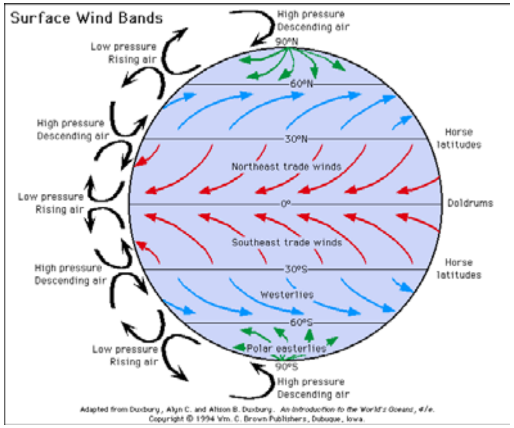

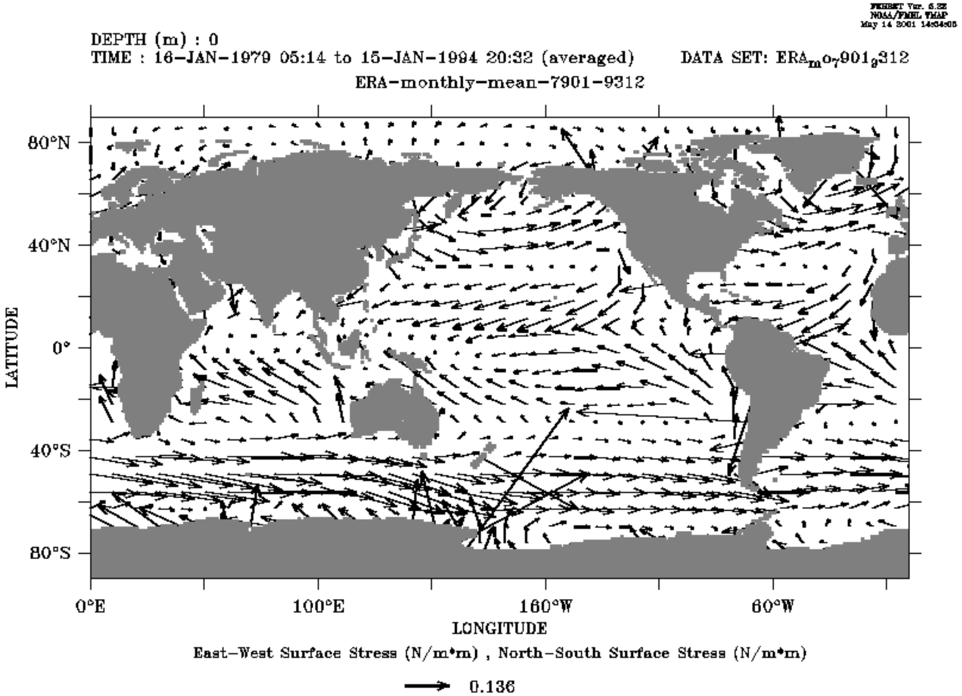

Wind-driven circulation (2)

In a steady state, the conservation of horizontal momentum in the surface layer, (u_E, v_E), can be simplified to a balance between the Coriolis accelaration and the acceleration due to stress:

$$-f v_E = \frac{1}{\rho_0}\frac{\partial \tau_x}{\partial z} \quad \text{and} \quad f u_E = \frac{1}{\rho_0}\frac{\partial \tau_y}{\partial z}$$

where **$f = 2\,\Omega\,\sin(\varphi)$** is the Coriolis parameter. Integrating from a depth h, where the stress becomes negligibly small, to the surface results in the following equation for the <u>vertical mean, horizontal mass transport</u>:

$$\vec{M}_{hor} = \left(+\frac{1}{f}\tau_y\,,\; -\frac{1}{f}\tau_x\right)$$

which shows that the mass transport is <u>perpendicular</u> to the surface stress, to the right of τ in the northern hemisphere, to the left in the sourthern hemisphere.

Because momentum is dissipated through internal friction, the wind-induced stress can penetrate only to a finite depth into the ocean. This depth defines the <u>Ekman layer</u>. The associated mass transport is therefore also called <u>Ekman transport</u>.

Wind-driven circulation (3)

A depiction of the various mechanisms acting in the Ekman layer is provided with the following picture.

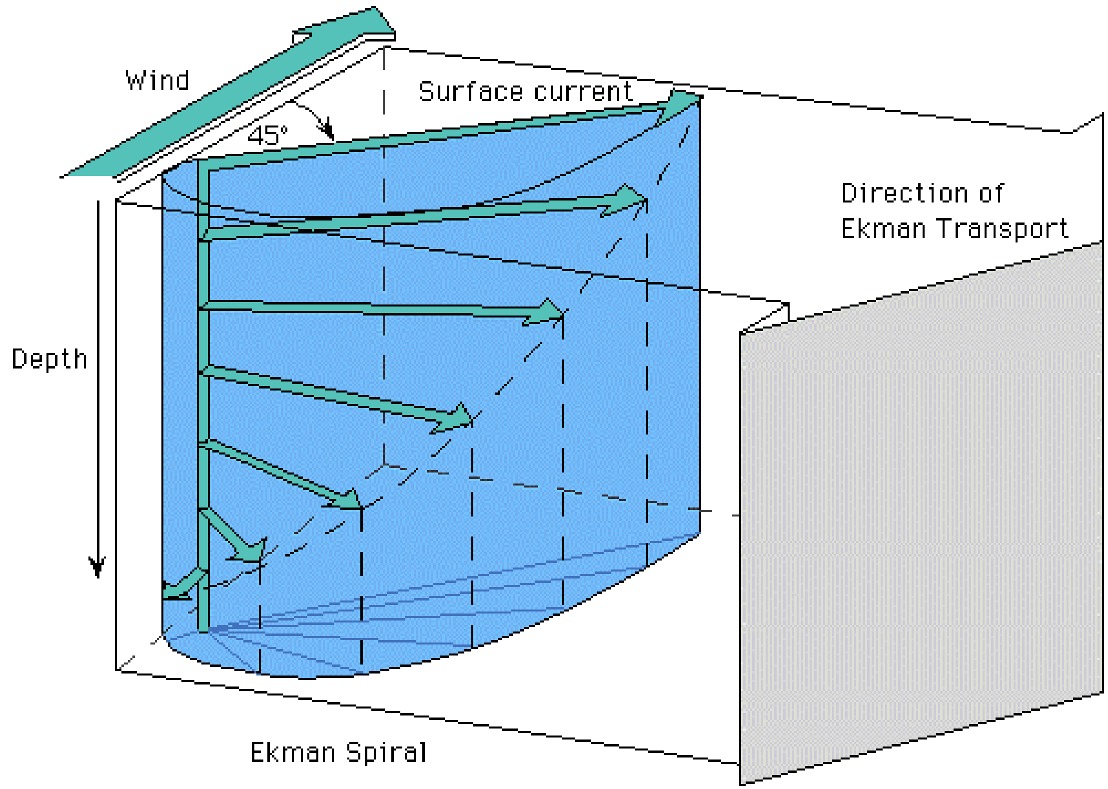

Adapted from Thurman, Harold V. **Essentials of Oceanography, 5th ed.** Prentice-Hall, Inc., 1996.

Ekman up- and downwelling

Depending on whether the Ekman transport in a given area is convergent or divergent, there is an associated vertical transport which is directed downward or upward. Associated vertical velocities are generally less than 0.5 m s^{-1}, but they nevertheless significantly contribute to the vertical motion in the upper ocean.

A well known example of vertical motion driven by the surface stress is the upwelling of cold water along the coast of Peru. This is an important component of the El Niño / La Niña phenomenon.

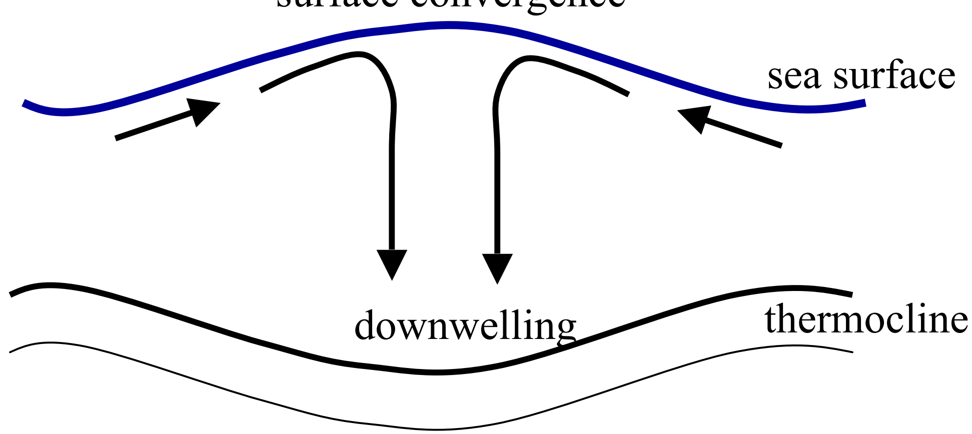

Equatorial upwelling

In the equatorial regions the divergence of the Ekman transport leads to a steady upwelling, that is apparent in the distribution of the water temperature.

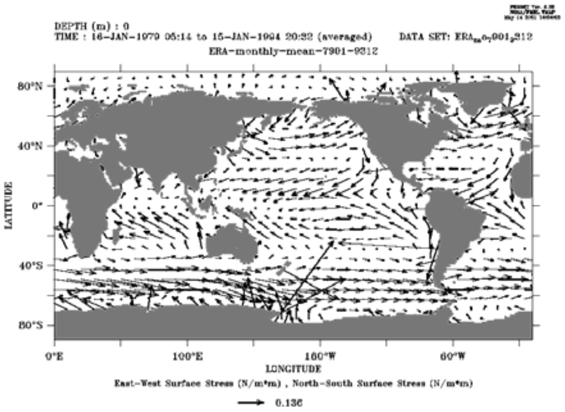

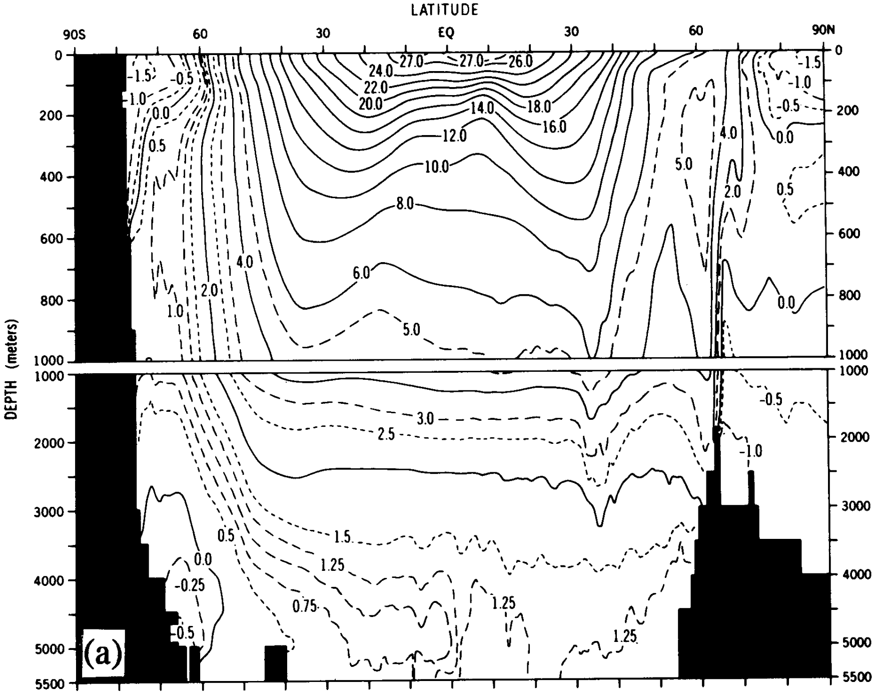

Hartmann (1991)

The gyres

<u>Rotational structures</u> in the surface currents are apparent in many areas of the world oceans. These rotational structures are called <u>gyres</u>.

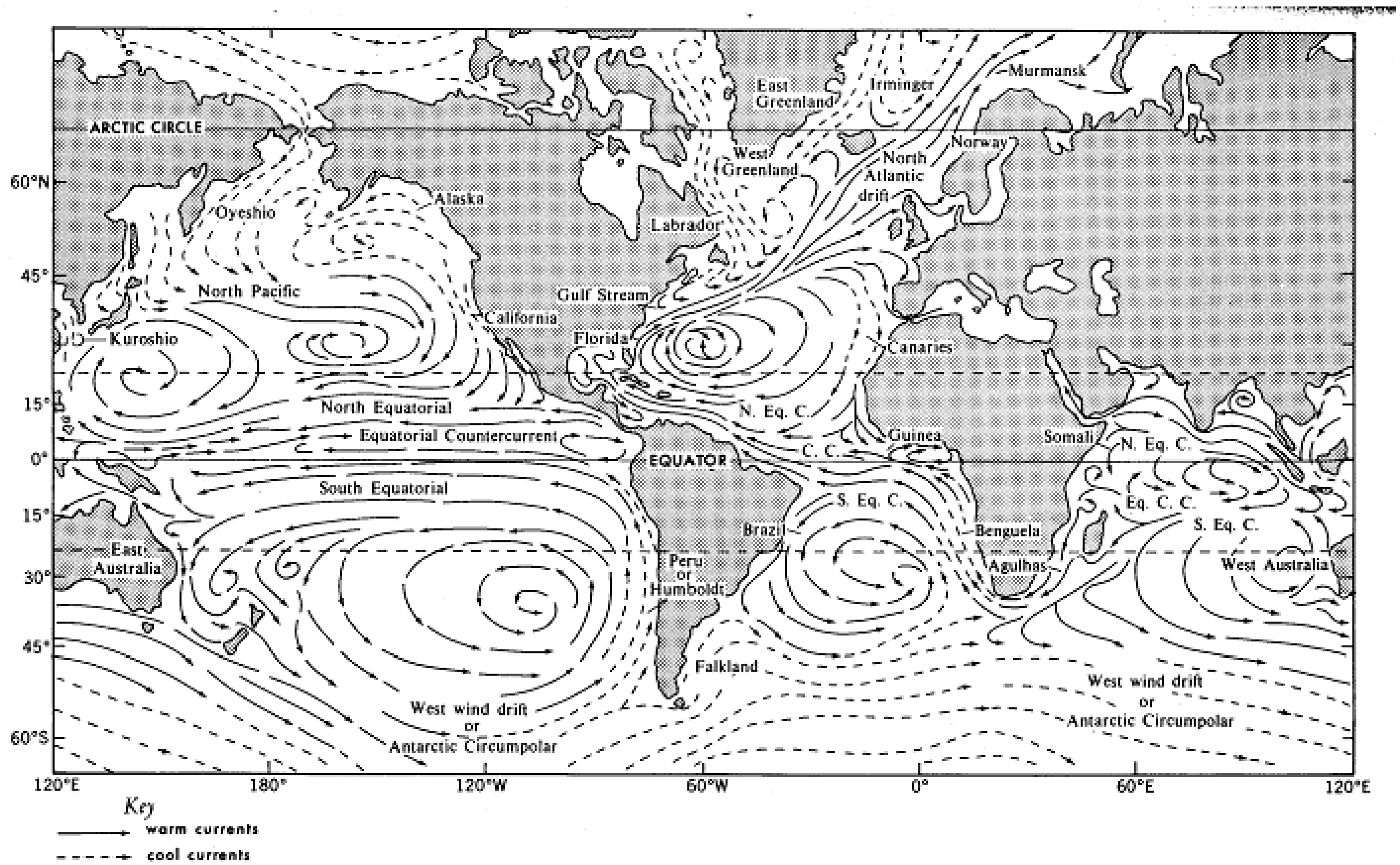

Trenberth (1992)

The gyres (2)

Schematically the gyre circulation can be represented as follows.

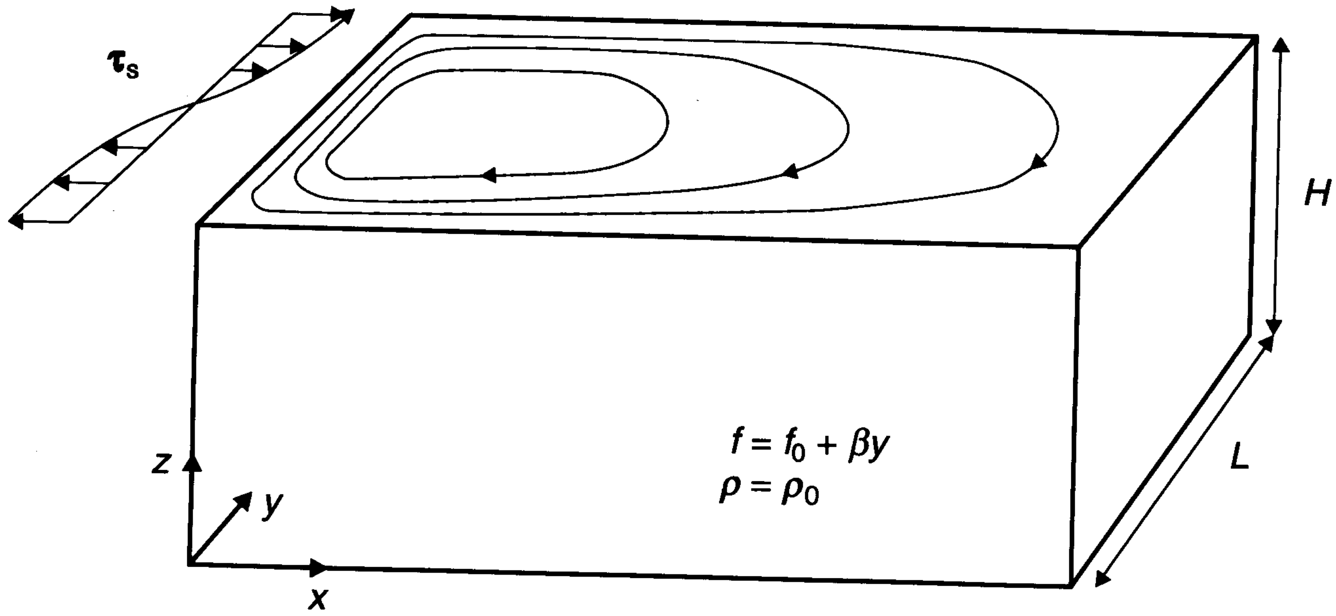

The gyres (3)

The dynamics of the gyres can be understood in terms of the conservation of potential vorticity in a basin of limited size:

$$\frac{\zeta + f}{H}$$

where f is the Coriolis parameter, H the depth of the layer and ζ is the relative vorticity defined in terms of the east- and northward components of the current, u and v, as:

$$\zeta = \frac{\partial v}{\partial x} - \frac{\partial u}{\partial y}$$

A derivation of the relevant equations can be found in e.g. Pond and Pickard (1983). We note that the relative vorticity can be changed by moving in the meridional direction (change in f), varying the depth H of the water layer, but also due to frictional effects, in particular at the eastern and western boundaries of the oceanic basins.

The gyres (4)

For a symmetric circulation across the oceanic basins (intensity of the meridional current on the western side equal to the intensity of the current on the eastern side), the forcing terms would not balance, leading to a steady acceleration of the gyre.

However, a steady state is possible by allowing a strong western boundary current trapped in a narrow zone near the coast. The Gulf Stream in the North Atlantic and the Kuroshio Current in the North Pacific are examples of such a current.

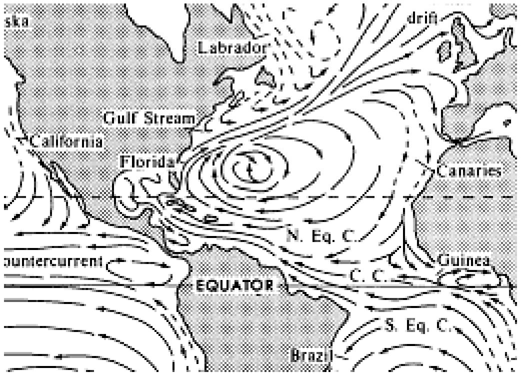

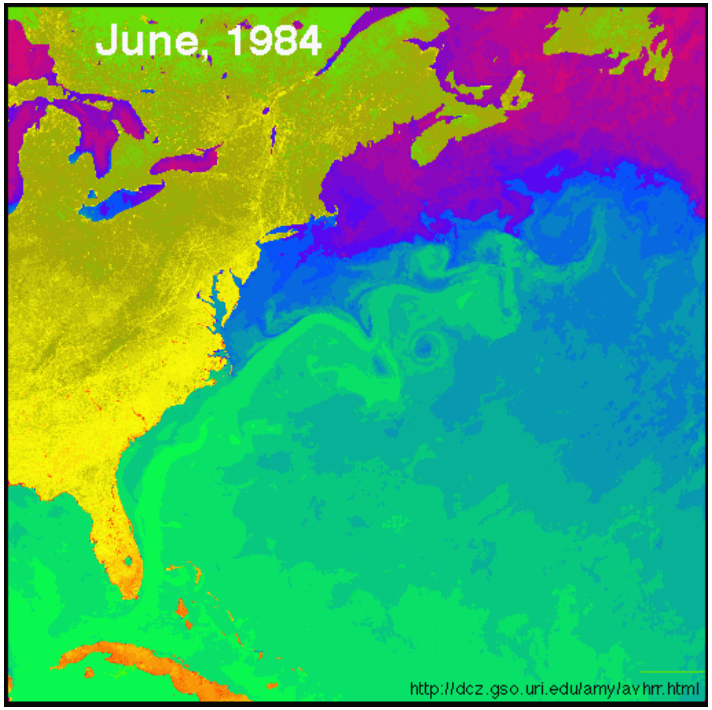

The thermohaline circulation

The global circulation of the world oceans is known as the thermohaline circulation. It is driven by density gradients that are due to variations in temperature and salinity. A schematic of the thermohaline circulation as proposed by Broecker (1987) is shown in the following figure. Surface currents are in red, depp currents in blue. The main sources of deep water in the North Atlantic and the Southern Ocean are indicated with yellow dots.

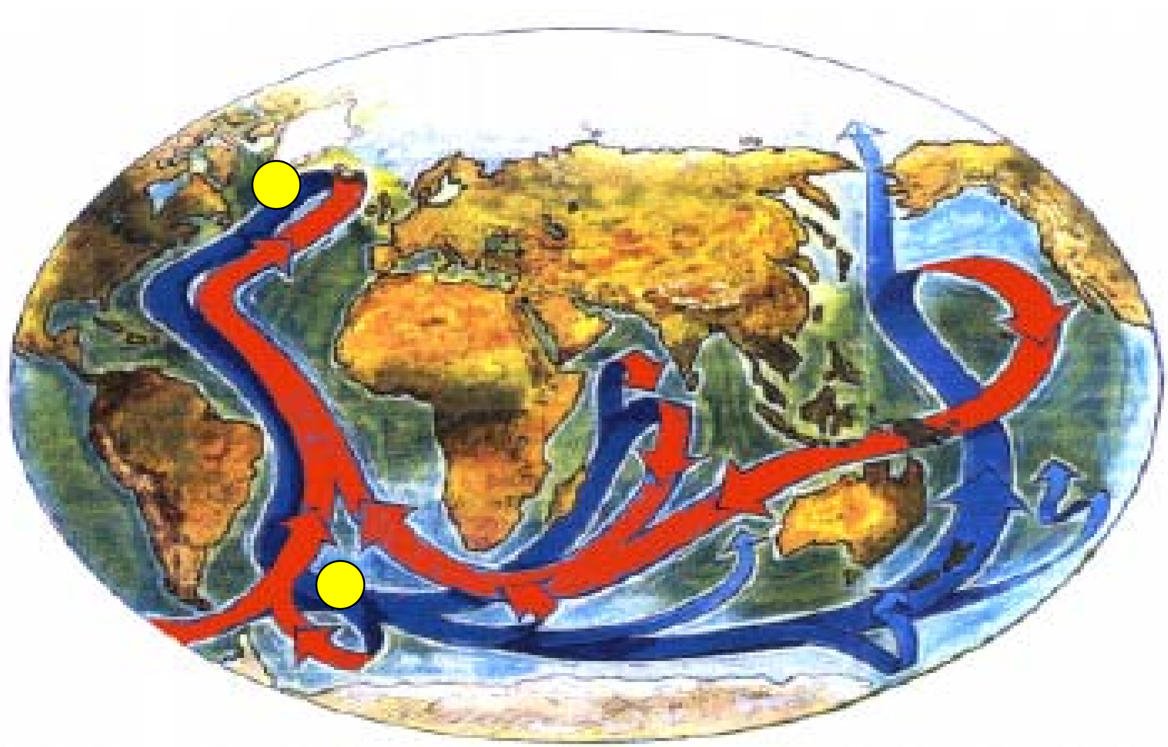

Formation of deep water in the North Atlantic

One of the two main sources of deep water is located in the North Atlantic. The densification of the surface water on the northward side of the Gulf Stream occurs through three processes:

- cooling (mainly in winter) through evaporation and longwave radiation;
- loss of fresh water through evaporation;
- salt rejection during seaice formation;
- the transport of salty water into the North Atlantic.

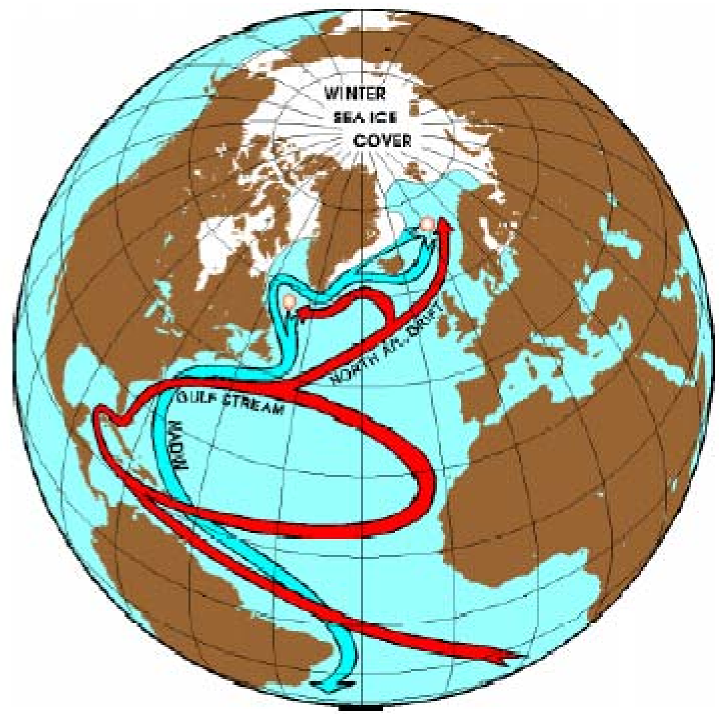

Fig. 3. The Atlantic Conveyor Belt. Orange circles show the regions of convection in the Greenland/Norwegian and Labrador Seas. The outflow of North Atlantic Deep Water (NADW) is shown in blue.

Rahmstorf (1999)

As speculated by Rahmstorf (1999) evaporation is not really needed to maintain the coveyor belt in the North Atlantic. The transport of salty water is much more important.

The key factor: salinity

Why is there no deep water formation in the North Pacific?

Obviously the density of water in this basin is not sufficiently high to induce penetration of surface water to the bottom of the ocean. The absence of cooling is certainly not the main reason: the waters of the North Pacific are cold.

What is really missing is salinity. The North Pacific is definitely less salty then the North Atlantic (an average of 32 ‰ as compared to 35 ‰).

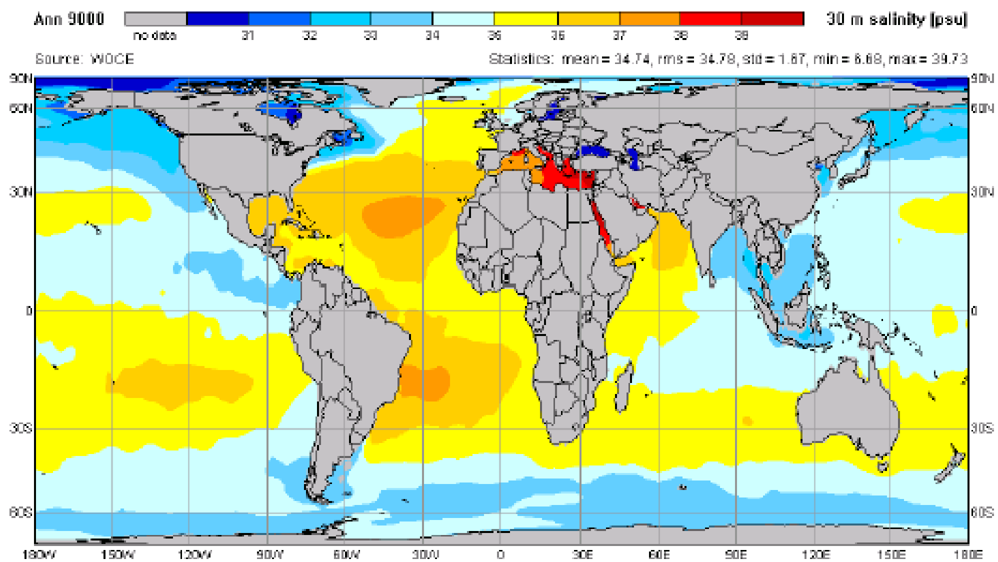

Fig 14.16 Global distribution of salinity at 30 m depth in the global ocean based on the WGHC climatology

Koltermann et al. (2005)

The thermohaline circulation and climate change

The state of the thermohaline circulation can change abruptly, as demonstrated by proxy records of past climatic changes. The supply of fresh water in the North Atlantic from melt water and icebergs during the final stage of a glacial cycle is one of the main reasons for the temporary shut down of the conveyor belt. More on this topic later on.